Supporting Information

Facile Synthesis of Oxidized Activated Carbon for High-Selectivity and Low-Enthalpy CO_2 Capture from Flue Gas

Ziyin Li,[a] Xiuling Ma,[a] Shunshun Xiong,[c] Yingxiang Ye,[a] Zizhu Yao,[a] Quanjie Lin,[a] Zhangjing Zhang,*[,a,b] and Shengchang Xiang*[,a,b]

[a] College of Chemistry and Materials Science, Fujian Provincial Key Laboratory of Polymer Materials, Fujian Normal University, 32 Shangsan Road, Fuzhou 350007, PR China

[b] State Key Laboratory of Structural Chemistry, Fujian Institute of Research on the Structure of Matter, Chinese Academy of Sciences, Fuzhou, Fujian 350002, PR China

[c] Institute of Nuclear Physics and Chemistry, China Academy of Engineering Physics, Mianyang, Sichuan 621900, PR China

Contents

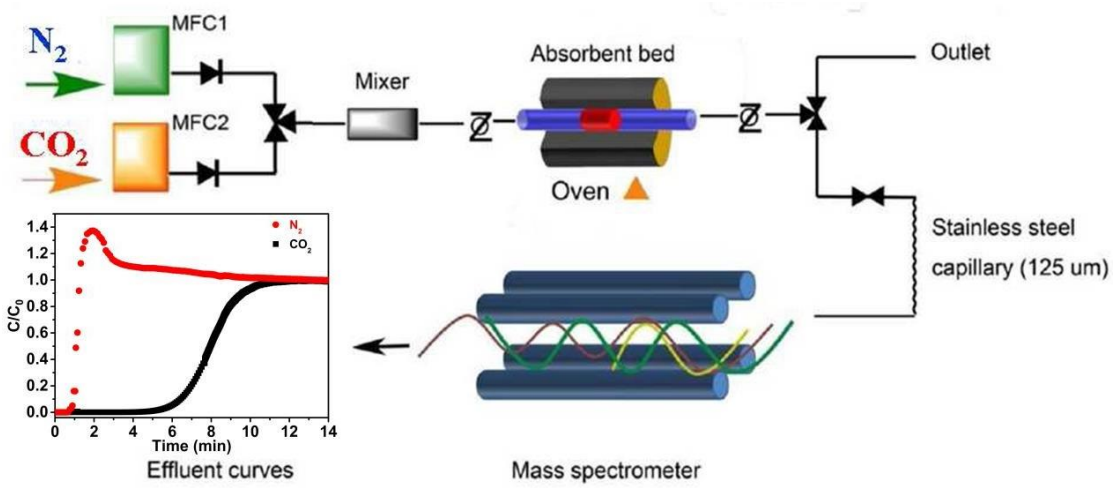

Scheme S1 Illustration of a lab-scale fix-bed reactor.

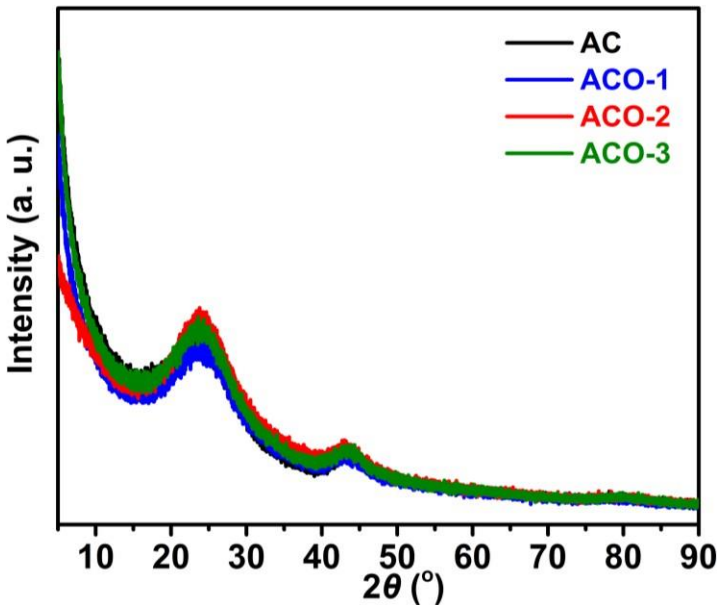

Fig. S1 PXRD patterns of AC, ACO-1, ACO-2, and ACO-3.

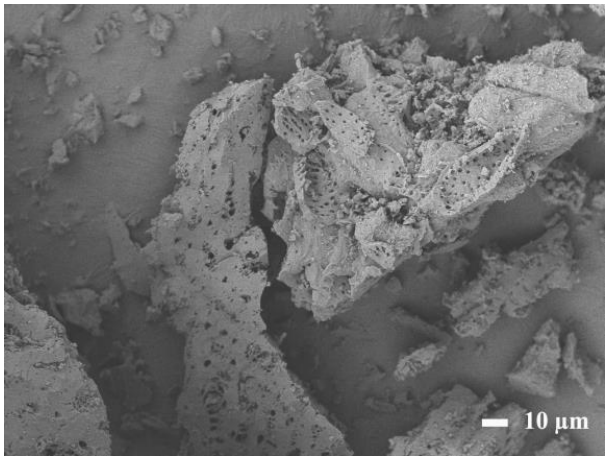

Fig. S2 SEM images of AC with 500 fold magnification.

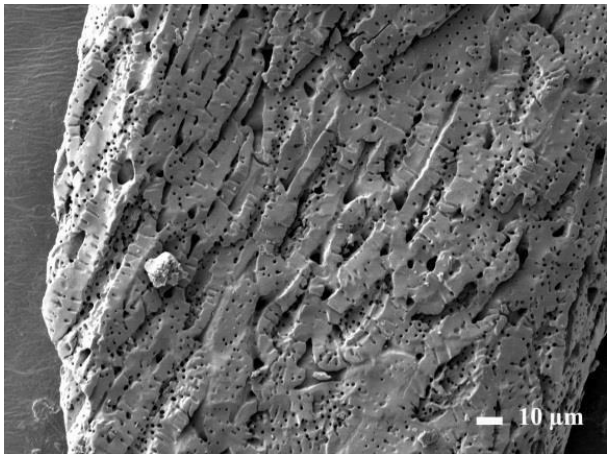

Fig. S3 SEM images of ACO-1 with 500 fold magnification.

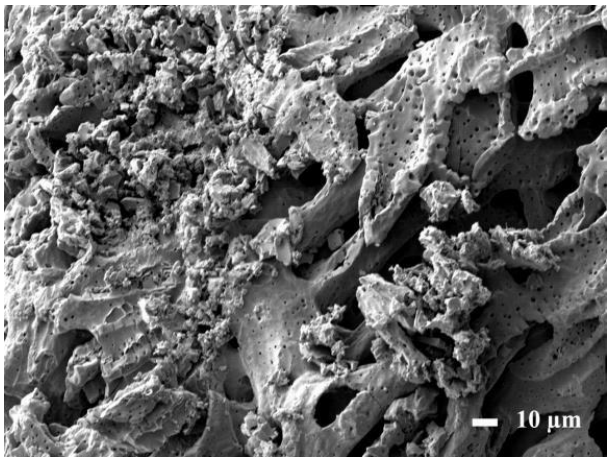

Fig. S4 SEM images of ACO-3 with 500 fold magnification.

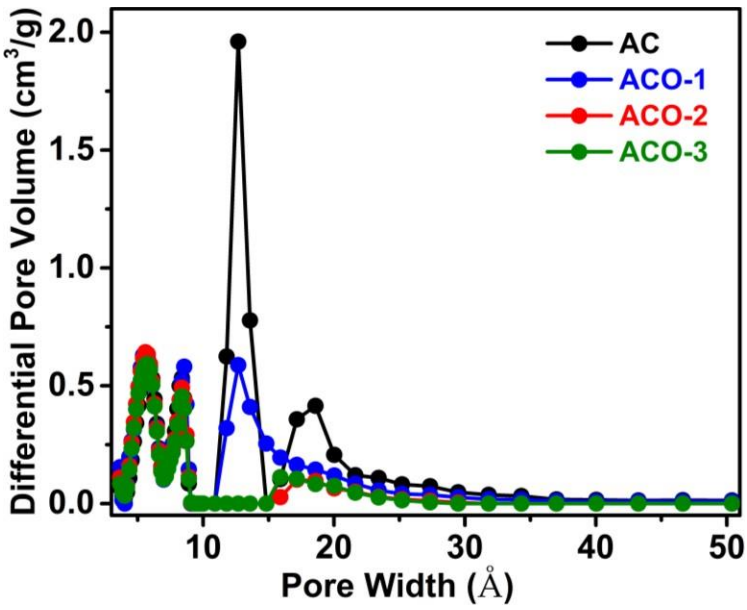

Fig. S5 Pore-size distribution of AC, ACO-1, ACO-2, and ACO-3 calculated by the non-local density functional theory (NLDFT).

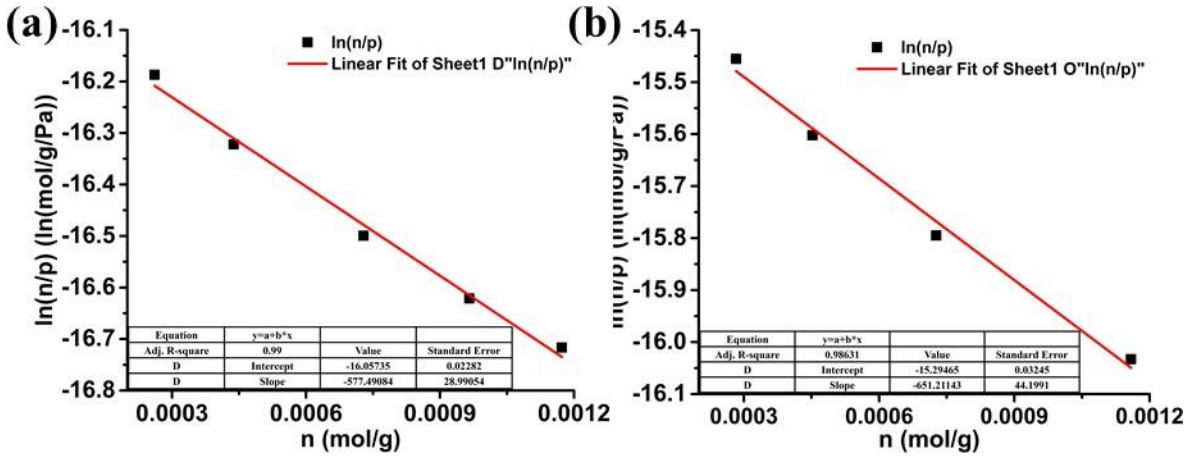

Fig. S6 The virial graphs for adsorption of CO_2 on AC at 296 K (a) and 273 K (b).

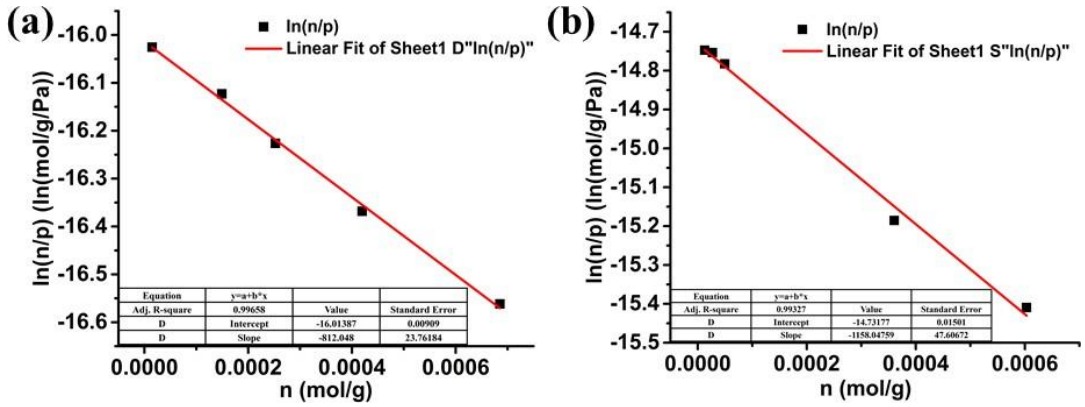

Fig. S7 The virial graphs for adsorption of CO_2 on ACO-1 at 296 K (a) and 273 K (b).

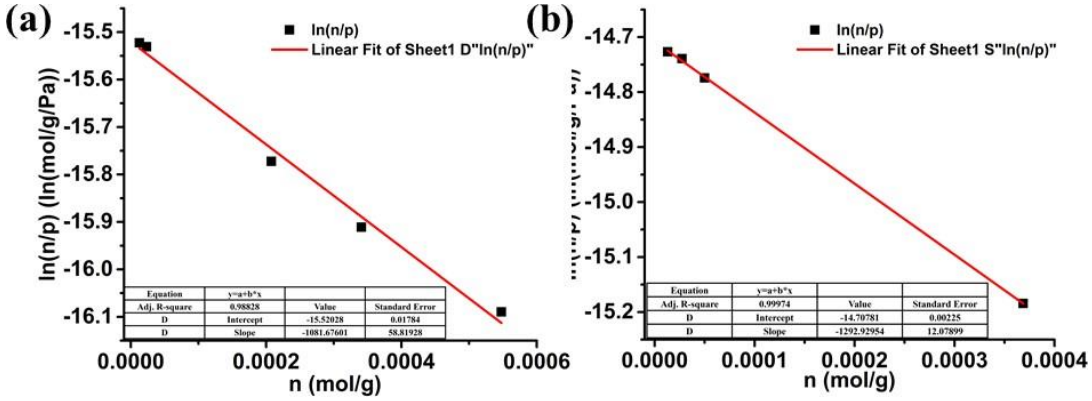

Fig. S8 The virial graphs for adsorption of CO_2 on ACO-2 at 296 K (a) and 273 K (b).

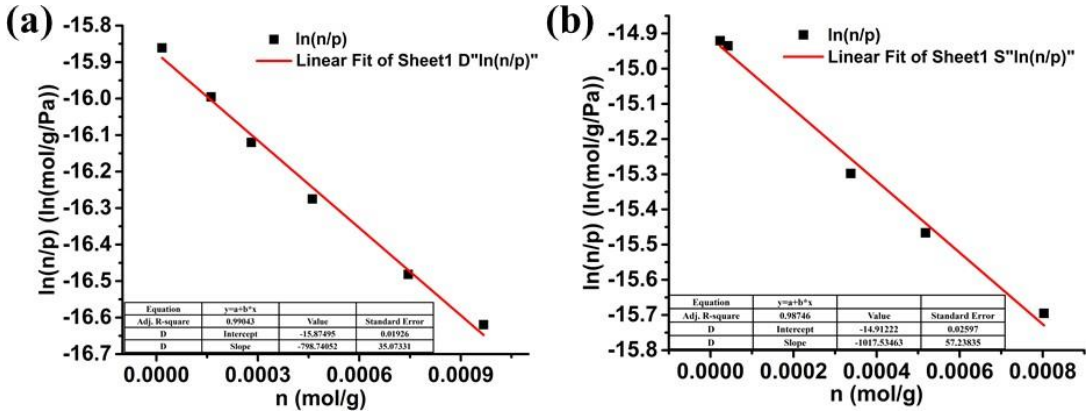

Fig. S9 The virial graphs for adsorption of CO_2 on ACO-3 at 296 K (a) and 273 K (b).

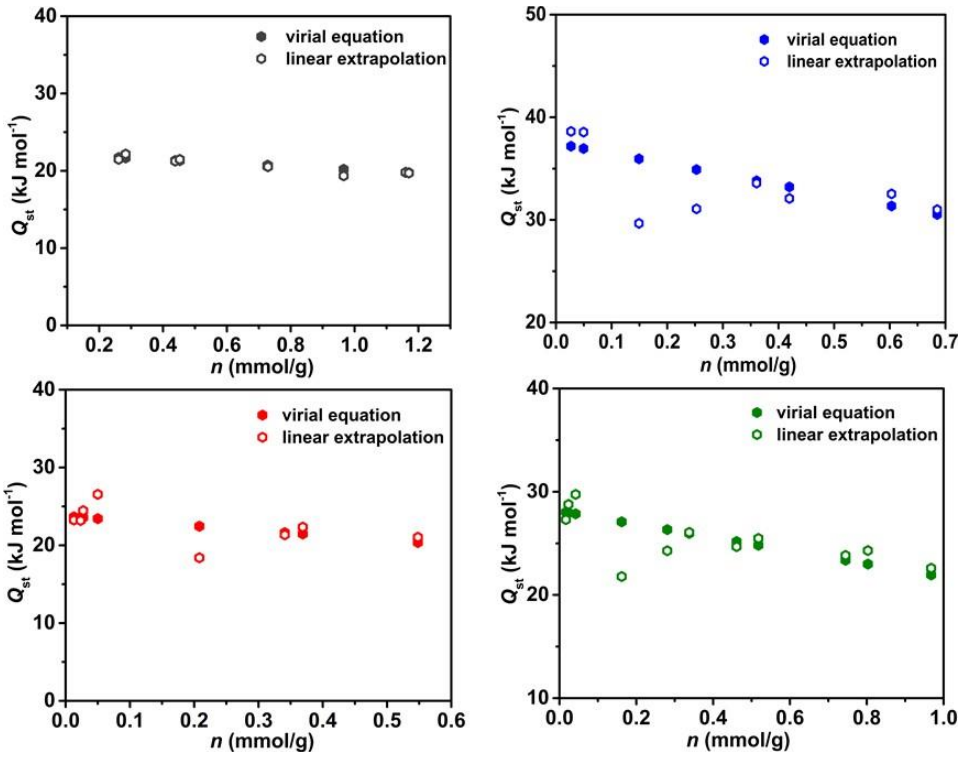

Fig. S10 Comparison of the enthalpies for gas adsorption of CO_2 on AC (gray), ACO-1 (blue), ACO-2 (red), and ACO-3 (olive green) from two methods: virial equation (solid) and linear extrapolation (open).

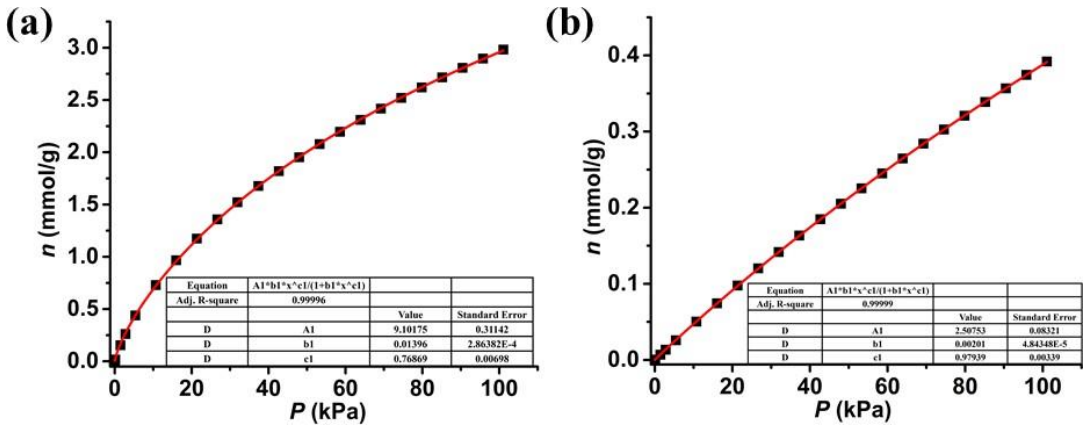

Fig. S11 The graphs of the Single-site Langmuir-Freundlich equations fit for adsorption of CO_2 (a), N_2 (b) on AC at 296 K.

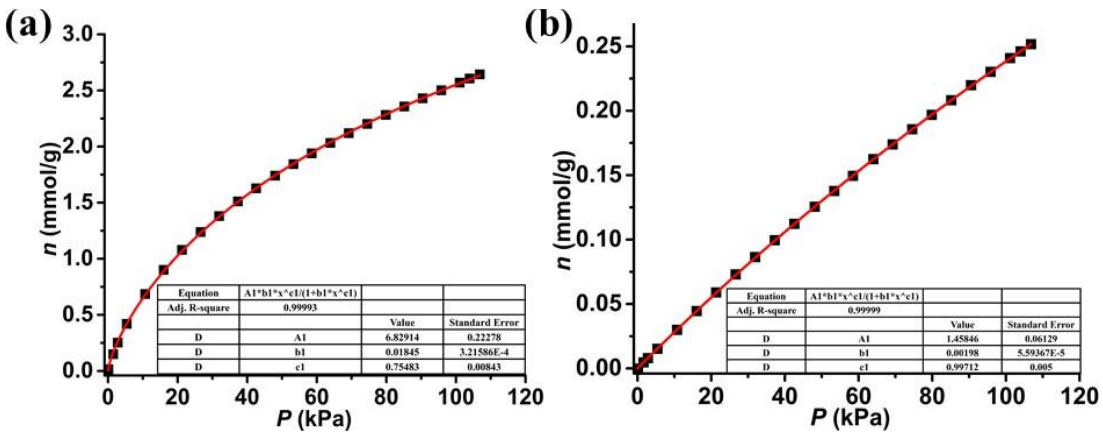

Fig. S12 The graphs of the Single-site Langmuir-Freundlich equations fit for adsorption of CO_2 (a), N_2 (b) on ACO-1 at 296 K.

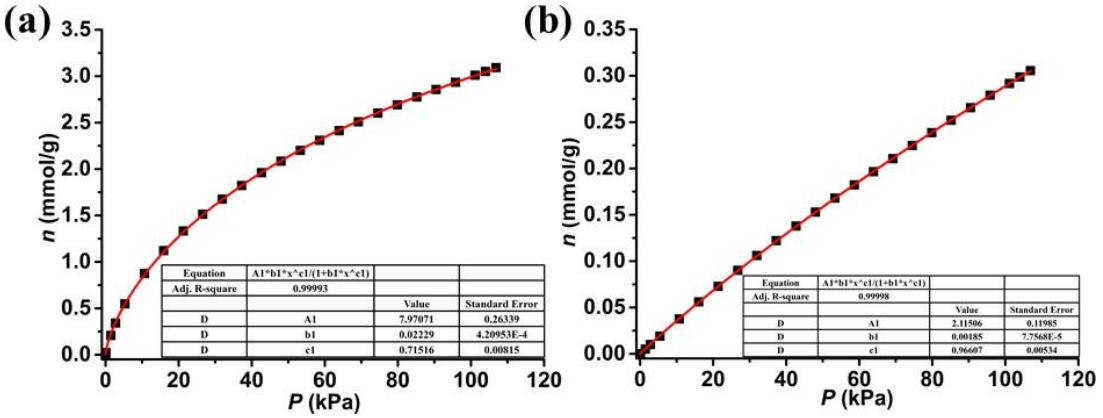

Fig. S13 The graphs of the Single-site Langmuir-Freundlich equations fit for adsorption of CO_2 (a), N_2 (b) on ACO-2 at 296 K.

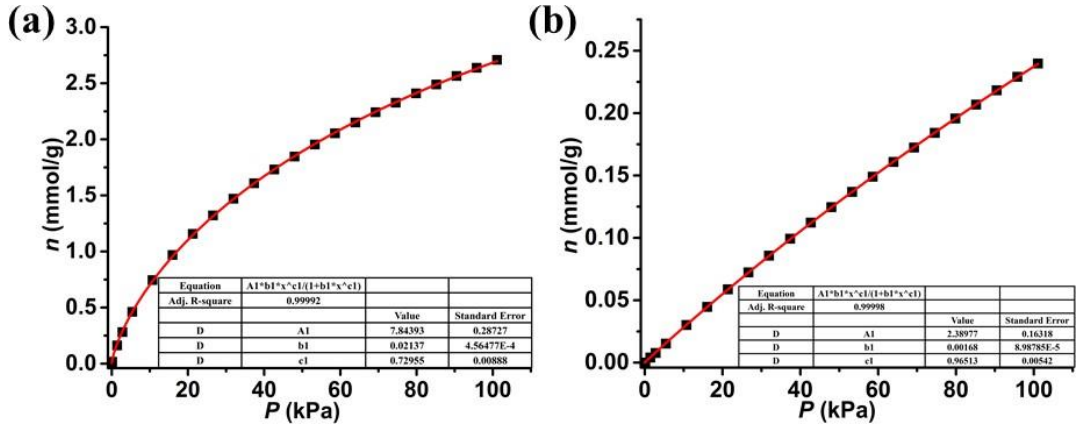

Fig. S14 The graphs of the Single-site Langmuir-Freundlich equations fit for adsorption of CO_2 (a), N_2 (b) on ACO-3 at 296 K.

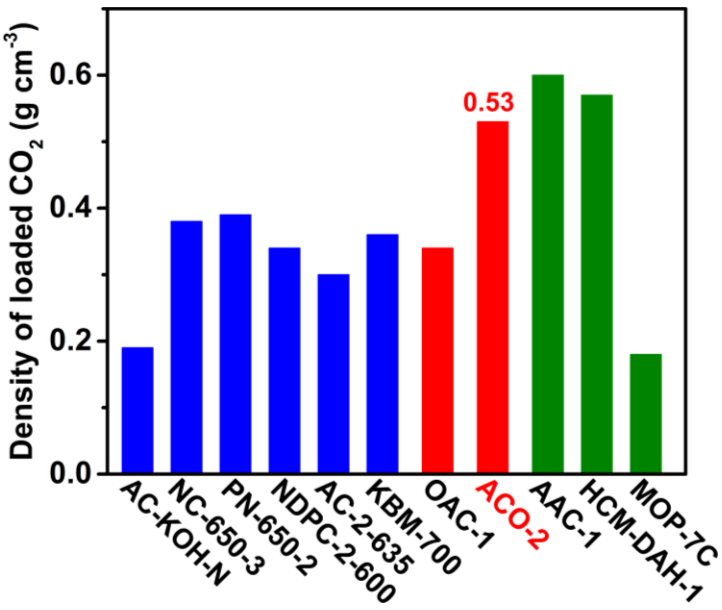

Fig. S15 The comparison of loaded CO_2 density on ACO-2 with representative porous carbon materials. Green (blue) bars represent representative porous carbons that modification with different method such as N doping, K^+ ions doping and carbonization, while red bars express the porous carbons were modification by O doping which are showing in Table S2.

Table S1 Porous structure parameters of the AC and ACO-n samples.

Sample	S_{BET} [a] (m^2/g)	S_{Lang} [b] (m^2/g)	V_p [c] (cm^3/g)
AC	948.63	1259.73	0.28
ACO-1	805.14	920.66	0.24
ACO-2	832.05	981.51	0.25
ACO-3	657.21	811.02	0.23

[a]The specific surface area was determined by the BET equation (p/p_0 = 0.05−0.3).

[b]The specific surface area was determined by the Langmuir quation (p/p_0 = 0.05−0.98).

[c]The micropore volume were estimated by Dubinin-Radushkevich (DR) method (eq. S1) in relative pressure range from 10^{-4} to 10^{-2} based on the adsorption isotherms of CO_2 at 273 K.[1]

$$V/V_0 = exp\left(-1/(E_0\beta)^2\left(RTln(p/p_0)\right)^2\right) \quad \text{(eq. S1)}$$

where V is the volume adsorbed at a pressure p, V_0 is the micropore volume, E_0 is the characteristic energy dependent on the pore structure, and β is the affinity coefficient which is characteristic of the adsorptive. The term $\left(RTln(p/p_0)\right)^2$ is usually named A^2.

Table S2 The comparison of CO_2 adsorption performances on ACO-2 with representative porous carbon materials.

Materials	Modification method	CO_2 uptake 296 K, 1 bar (mmol/g)	BET ($m^2\ g^{-1}$)	Q_{st} (kJ/mol)	IAST	V_p (cm^3/g)	ρ [a] (g/cm^3)	Refs
AC-KOH-N	KOH, N doping	5.05	2511	33.6	30.75	1.16	0.19	2
NC-650-3	KOH, N doping	4.80	1535	33.0	19[b]	0.56	0.38	3
PFS-800	KOH	4.62	1272	40.0	-	0.38	0.53	4
PN-650-2	KOH, N doping	4.57	1445	37.0	22[b]	0.52	0.39	5
PUF-400-KOH-1-700	KOH	4.33	1516.3	61.0	-	0.57	0.33	6
NDPC-2-600	N doping	4.30	1211	74.2	15.2	0.55	0.34	7
KNC-A-K	KOH, N doping	4.04	614	59.3	48[b]	-	-	8
NPC-2	KOH, N doping	4.02	1255.9	33.5	32.4	0.52	0.34	9
AC-2-635	K_2CO_3	3.86	1381	30.4	21	0.56	0.30	10
mJUC160-900	N doping	3.50	940	23.1	29	0.34	0.45	11
OAC-1	O doping	3.46	925	23.5	26.5	0.45	0.34	12
KBM-700	KOH, N doping	3.29	1129	44.0	99.1	0.40	0.36	13
NPC-650	KOH, N doping	3.10	1561	43.0	-	0.65	0.21	14
ACO-2	O doping	3.01	832.05	23.1	48.5	0.25	0.53	This work
AAC-1	Carbonization	3.00	392	28.0	45	0.22	0.60	15
MOFC-800	N doping	2.96	1086.9	28.1	29	-	-	16
HCM-DAH-1	N doping	2.60	670	35.9	28	0.20	0.57	17
MOP-7C	KOH, carbonization	2.23	1508	34.7	21	0.56	0.18	18
IBN9-NC1	N doping	1.81	925	44.1	42	0.16	0.50	19
MCN	N doping	1.46	156	32.2	158[b]	-	-	20

The porous carbons materials with orange and green background are modified by oxygen-doping.

[a] Calculated the density of loaded CO_2 by the equation

$$\rho = \frac{N_{(CO_2)} \times 44}{V_p \times 22.4 \times 1000} \qquad (8)$$

ρ is the density of loaded CO_2 ($g\ cm^{-3}$), and $N_{(CO2)}$ is CO_2 sorption capacity at 296 K and 1 bar ($cm^3\ g^{-1}$).

[b] The selectivity predicted by IAST for the gas mixtures (CO_2:N_2 = 0.10:0.90) at 296 K.

REFERENCES

1 (a) D. C. Amorós, J. A . Monge and A. L. Solano, *Langmuir*, 1996, ***12***, 2820–2824; (b) D. C. Amorós, J. A . Monge, M. A. C. Lillo and A. L. Solano, *Langmuir*, 1998, ***14***, 4589–4596.

2 C. M. Zhang, W. Song, Q. L. Ma, L. J. Xie, X. C. Zhang and H. Guo, *Energy & Fuels*, 2016, ***30***, 4181–4190.

3 J. Chen, J. Yang, G. S. Hu, X. Hu, Z. M. Li, S. W. Shen, M. Radosz and M. H. Fan, *ACS Sustainable Chem. Eng.*, 2016, ***4***, 1439−1445.

4 P. Li, C. Xing, S. J. Qu, B. Li and W. Z. Shen, *ACS Sustainable Chem. Eng.*, 2015, ***3***, 1434−1442.

5 M. Yang, L. Guo, G. Hu, X. Hu, J. Chen, S. Shen, W. Dai and M. Fan, *Ind. Eng. Chem. Res.*, 2016, ***55***, 757−765.

6 C. Ge, J. Song, Z. F. Qin, J. G. Wang and W. B. Fan *ACS Appl. Mater. Interfaces*, 2016, ***8***, 18849−18859.

7 N. Fu, H. M. Wei, H. L. Lin, L. Li, C. H. Ji, N. B. Yu, H. J. Chen and G. Y.Xiao, *ACS Appl. Mater. Interfaces*, 2017, ***9***, 9955−9963.

8 Y. F. Zhao, X. Liu, K. X. Yao, L. Zhao and Y. Han, *Chem. Mater.*, 2012, ***24***, 4725−4734.

9 L. Wan, J. L. Wang, C. Feng, Y. H. Suna and K. X. Li, *Nanoscale*, 2015, ***7***, 6534–6544.

10 X. Q. Fan, L. X. Zhang, G. B. Zhang, Z. Shu and J. L. Shi, *Carbon*, 2013, ***61***, 423–430.

11 Y. Pan, M. Xue, M. Chen, Q. Fang, L. Zhu, V. Valtcheva and S. L. Qiu, *Inorg. Chem. Front.*, 2016, ***3***, 1112–1119.

12 J. Wang, R. Krishna, J. F, Yang and S. G. Deng, *Environ. Sci. Technol.*, 2015, ***49***, 9364–9373.

13 Y. Pan, Y. X. Zhao, S. J. Mu, Y. Wang, C. M. Jiang, Q. Z. Liu, Q. R. Fang, M. Xue and S. L. Qiu, *J. Mater. Chem. A*, 2017, ***5***, 9544–9552.

14 J. C. Wang, I. Senkovska, M. Oschatz, M. R. Lohe, L. Borchardt, A. Heerwig, Q. Liua and S. Kaskel, *J. Mater. Chem. A*, 2013, ***1***, 10951–10961.

15 J. Wang, J. F. Yang, R. Krishna, T. Yang and S. Deng, *J. Mater. Chem. A*, 2016, ***4***, 19095–19106.

16 L. J. Li, Y. Wang, X. Gu, Q. P. Yang and X. B. Zhao, *Chem. Asian J.*, 2016, ***11***, 1913–1920.

17 G. P.; Hao, W. C. Li, D. Qian, G. H. Wang, W. P. Zhang, T. Zhang, A. Q. Wang, F. Schüth, H. J. Bongard and A. H. Lu, *J. Am. Chem. Soc.*, 2011, ***133***, 11378–11388.

18 S. Gu, J. Q. He, Y. L. Zhu, Z. Q. Wang, D. Y. Chen, G. P. Yu, C. Y. Pan, J. G. Guan, K. Tao, *ACS Appl. Mater. Interfaces*, 2016, ***8***, 18383−18392.

19 Y. F. Zhao, L. Zhao, K. X. Yao, Y. Yang, Q. Zhang, Y. Han, *J. Mater. Chem.*, 2012, ***22***, 19726–19731.

20 D. Li, Y. Chen, M. Zheng, H. Zhao, Y. Zhao, Z. Sun, *ACS Sustainable Chem. Eng.*, 2016, ***4***, 298−304.